IEEE Access
Multidisciplinary ⁝ Rapid Review ⁝ Open Access Journal

Received 22 August 2023, accepted 17 September 2023, date of publication 25 September 2023, date of current version 2 October 2023.

Digital Object Identifier 10.1109/ACCESS.2023.3318723

RESEARCH ARTICLE

Cooperative Control of Recurrent Neural Network for PID-Based Single Phase Hotplate Temperature Control Systems

SONG XU[1], **(Member, IEEE), SIYUAN SHI**[1], **WEI JIANG**[2], **(Member, IEEE), AND SEIJI HASHIMOTO**[3], **(Member, IEEE)**

[1]School of Automation, Jiangsu University of Science and Technology, Zhenjiang 212100, China
[2]Department of Electrical Engineering, Yangzhou University, Yangzhou 225000, China
[3]Division of Electronics and Informatics, Gunma University, Kiryu 376-8515, Japan

Corresponding author: Song Xu (songxu@just.edu.cn)

This work was supported by the Natural Science Foundation of the Jiangsu University of Science and Technology under Grant 1032932101.

ABSTRACT High-precision temperature control technology is currently more and more important in industrial thermal processing systems. In this paper, an RNN controller with integral-proportional-derivative (IPD) compensation driven by a reference model is proposed for single phase hotplate temperature control systems. A reference model is introduced based on the real controlled plant for the RNN controller to obtain better self-learning and adjusting efficiency by providing a more valuable teaching signal. Further, an Adam optimization algorithm is applied to improve the control performance of the RNN controller. The simulations were developed under a MATLAB environment and the experiments were performed on a temperature experimental platform that used a digital-signal-processor (DSP) as digital controller. The results of simulations and experiments were quantitatively compared with those for a conventional temperature control system which only had an IPD controller. The control efficiency of the proposed RNN method was successfully evaluated.

INDEX TERMS Cooperative temperature control, recurrent neural network controller, Adam optimization algorithm, single phase hotplate temperature control.

14 **NOMENCLATURE**

x_N	RNN controller output.
α	Gain of weight training and updating.
α_{ad}	Step size of *Adam* calculation.
β	Ratio of bias training and updating.
$\delta_h(n)$	Local gradient of hidden layer.
$\delta_o(n)$	Local gradient of output layer.
η	Gain of the low-pass filter.
τ	Pure delay time.
b	Offset value of the neurons in hidden layer.
C	Conventional PID controller.
c	Bias of the neurons in the output layer.
15 C_{NN}	Recurrent neural network controller.
e_y	Error between the output of reference model and the real output temperature.
$f(\cdot)$	Activation function of each neurons in the RNN controller.
F_{out}	Output of the feedforward compensator.
FF	Feed forward compensator.
K	Steady state gain.
K_p	Proportional gain of the controller.
m	Number of output layer neurons.
N_{in}	Input of neural network controller.
N_{out}	Output of neural network controller.
$o(n)$	Induced local domain of the output layer.
$P(s)$	Controlled object.
R_m	Output of reference model.
T	Time constant.
T_d	Differential time constant. 16

The associate editor coordinating the review of this manuscript and approving it for publication was Min Wang.

T_i	Integral time constant.
U	Weight of input neurons.
$u(n)$	Induced local domain of the hidden layer.
V	Weight of output neurons.
W	State memory neurons' weight.
$w(n)$	Gradients of the neuron.
x	Sum of x_N and x_C.
x_C	PID output.
y	Error between the output of reference model.
y_{ref}	Set reference value for the system.
${e_y}^2$	Self-learning signal for the RNN controller.

I. INTRODUCTION

With the rapid development of artificial intelligence (AI), the application of this technology to industrial processes are becoming increasingly popular, with demands for control systems with optimal processing ability unprecedentedly high. Temperature control systems, as one part of industrial thermal processes, play a significant role in industrial applications, especially in semiconductor industrial and food processing such as water heating system temperature control, and hotplate baking temperature control. There are already many existing control methods, among them, the most popular and commonly applied of which is the proportional-integral-derivative (PID) control method, due to its simplicity and applicability [1], [2].

For single phase hotplate temperature control systems, the temperature needs to keep constant in different level and remain for a certain period of time. Normally the main difficulties in providing a precise, controlled temperature are the non-linearity, long response time, and large time delay of the controlled objects [3]. Hence, the temperature control system is becoming more and more complex, and strict requirements cannot be met by only using conventional control methods [4], [5]. Thus, the precise temperature control system difficulty for the hotplate temperature heating system can be conclude as follows:

- The controlled object has strong non-linearity, large response time and large time lag which results in uncontrollable feedback efficiency for precise control.
- The temperature system with uncertainty parameters, which will cause the timely change response characteristics.
- The hotplate temperature systems have strong disturbance, the control system needs to have the robustness for disturbance and keep the plate at a constant temperature.

In order to achieve precise temperature control, researchers prefer to build a mathematical model through a system identification method to analyze the response characteristics of the controlled system, and while they have proposed many identification methods, the most popular is the step-response method [6], [7], [8], [9].

An improved compensation method of the temperature control system can be developed based on a mathematical model. Ko has tried to introduce fuzzy logic into the proportional-integral control method to improve the conventional PI control efficiency [10]. Vicente and Raul have introduced the Smith estimation methods for the dead time compensation for a time delay plant [11]. Bai has developed the self-adaption control method for the plant with parameter disturbance [12]. Xu has proposed a predictive control method for comparison between real-time output and theoretical output [13]. Zhang performed the same research as Ko by introducing the fuzzy control method to improve control efficiency [14]. Afram introduced the model-predictive-control (MPC) which is suitable for systems with a precise mathematical model [15].

However, for the model-based advanced control method, the typical problem is that, once the parameters are defined, the control system cannot be changed while operating. For the temperature control system, the drawbacks of the controlled plant are very common and serious, and will lead to unstable operating control systems.

Recently, the effectiveness of artificial neural networks (ANNs), which are now widely used in industrial processes, have been demonstrated in terms of computational processors for various associative operations, classification, data compression, combination problem solving, adaptive control, and so on. Recurrent neural networks (RNNs), as one type of ANNs, which can represent temporal dynamic behavior through their own feedback loops in neurons, have gained increasing attention for application of industrial processes [16], [17]. During the last two decades, the application of neural network (NN) control methods to temperature control systems has seen sustained growth, such as model prediction [18], the improvement of comfort indices [19], and data calculation and compression [20], [21], [22], [23], [24]. For single phase temperature control systems, the characteristics of strong non-linearity slow time response and large time delay will make the system difficult to control, and the control efficiency of the designed control method is focused on the transient response and overshooting of the controlled objects [25], [26], [27]. Furthermore, to improve the performance of the NN controller, especially the hyper-parameter training efficiency of the neural networks, many optimization and initialization methods have been proposed such as the Stochastic Gradient Descent (SGD) algorithm, $Nesterov'sacceleratedgradient$ (NAG)and the Adam optimization algorithm [28], [29], [30]. Moreover, activation functions such as $Tanh$, $Sigmoid$, $Swvish$, $ReLu$ [31], [32], [33], [34], have been developed and optimization methods for the initial value of hyper-parameters have been introduced, such as *Zero initialization, Random initialization, He initialization* and *Xavier initialization* [35], [36], [37], [38].

Moreover, based on the machine learning technologies, the most latest researches have proposed different NN structure for control, the cooperation control such as feed-through Elman NN structure [39], Memory Recurrent Eman NN structure [40], and ANN based PID control strategies [41]. Although, there have existed a large amount research for

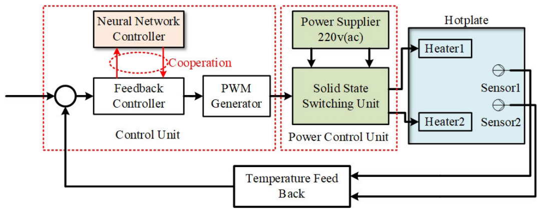

FIGURE 1. Overview of proposed hotplate temperature control system.

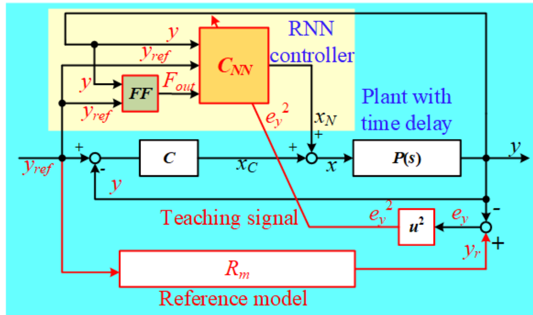

FIGURE 2. Block diagram of proposed reference-model-based recurrent neural network(RNN) control system.

efficiency control method [42], the application for those method in hotplate temperature control system still remains the following challenges.

- How to ensure the dynamic control stability of the NN controller for temperature system with large response time, big time lag and non-linearity characteristics.
- The proper hyper parameters of the NN controller suitable for the controlled object need to be trained.
- Due to the uncertainty of the hotplate parameters, the fast learning and model free ability of the NN controlled still need to be improved.

In view of the temperature control difficulties for hotplate system and challenges of the AI technology application. This manuscript, in order to realize precision temperature control, focused on improving the system response speed and reduce the overshoot of the single phase hotplate temperature control system which has the characteristics of strong non-linearity, long response time and large time delay, a recurrent neural network using Adam optimization method driven by a reference model is proposed. The RNN controller learns by using the squared error signal between the reference model output and the real system output. The Adam optimization algorithm is applied to improve the performance of the RNN, and a feed forward controller is introduced to provide an extra input for the RNN to learn and adjust the hyper parameters itself. The control input of the controlled object is obtained by the sum of the RNN controller output and the PID controller (IPD structure) output. The main contributions of this brief are summarized as follows:

- Cooperative RNN and IPD control structure using a normative model in which the NN learning satisfies the causal relationship (learning does not start before the input / output signal) even for the dead time control target.
- The proposed control structure realizes model free design, the IPD controller parameters are obtained by ZN method also the RNN hyper parameters can be designed without considering the controlled model.
- The proposed RNN controller is driven by reference model, also feed-forward compensation provides better learning reference for the RNN network and thus the RNN fast learning can be realized.

The rest of this paper is structured as follows: Section II details the structure of the proposed RNN control system part by part. Section III introduces the identification results of the controlled object and the simulation results, which are quantitatively compared with an IPD system. Section IV explains the experimental results of the control system, and quantitatively compares them with the results obtained from an IPD control system. Lastly, Section V contains a brief conclusion to this paper.

II. COOPERATIVE RNN CONTROL SYSTEM CONFIGURATION

Figure 1 shows the overview of the proposed hotplate temperature control system, where the whole system includes three parts indicated by control unit, power control unit and hotplate with temperature feedback, the hotplate is heating by two resistance heaters which is driven by solid state switching unit, and the solid state switching unit is controlled by PWM duty cycle generated by the control unit which implements the proposed cooperative RNN with PID control system.

As shown in Figure 1 the control unit is constructed by our proposed cooperative RNN control system, the block diagram of the proposed single phase hotplate temperature contol system which is driven by reference model obtained from a real hotplate temperature plant is shown in Figure 2.

For simplicity, the controlled object is expressed as a first order plus time delay(FOPTD) model. In Figure 2, C_{NN} indicates the recurrent neural network controller, while C is the conventional PID controller(IPD structure). y_{ref} is the set reference value for the system, e_y is calculated as the error between the output of reference model R_m and the real output temperature, and the squared error $e_y{}^2$ is used as the self-learning signal for the RNN controller, FF is the feed forward compensator that provides a reference control input of proportional-derivative (PD) or two-degree-of-freedom(2DOF) controllers for the RNN control to increase the learning efficiency of the RNN controller, C is a conventional PID controller (in this paper, an IPD configuration is employed), and x is the control input, which is the sum of the RNN controller output x_N and PID output x_C. R_m is the reference model which is used to provide a precise teaching signal for the RNN controller and is calculated based on the control object $P(s)$.

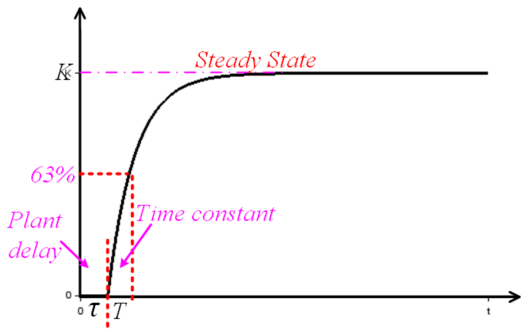

FIGURE 3. Step response of first order plus time delay (FOPTD) plant.

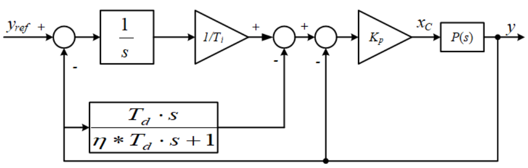

FIGURE 4. Block diagram of conventional proportional-integral-derivative (PID) control.

A. PLANT WITH PURE DELAY TIME

For single phase hotplate temperature control system in this proposal, the controlled object always has a large time constant and delay time. Thus, the object can be defined as a FOPTD system as in equation (28), where K is the steady state gain, T is the time constant, and τ is the pure delay time (also called dead time). The time response of the plant is shown in Figure 3.

$$P(s) = \frac{k}{Ts+1}e^{-\tau s}. \tag{1}$$

B. CONVENTIONAL PID CONTROLLER

Considering that the hyper parameters of the RNN controller need to be trained before the RNN controller works, the initial state of the SISO temperature system should be controlled, which is why the conventional PID controller is added for this purpose. The PID block diagram is presented in Figure 4, where T_i is the integral time constant, T_d is the differential time constant, η is the gain of the low-pass filter (LPF) used to control the differential part, and K_p is the proportional gain of the controller.

Stability is one of the most important factors of a controller. Several methods have been proposed for controller stability analysis [43], [44]. Because the parameters of the PID controller are designed based on the Ziegler-Nichols rule (step response method), stability is ensured [45]. These values are determined by τ, K and T in equation (1). The PID parameters K_p, T_i and T_d can be calculated as equations (2),(3) and (4), respectively.

Moreover, another important factor of a controlled system is the saturation of the actuator x. This proposal, the saturation is handled by setting saturation for the sum of PID output and NN output, and adding the saturation by subtracting it from the input of the PID controller (PID type normal anti-windup method). So that the actuator saturation can be avoided.

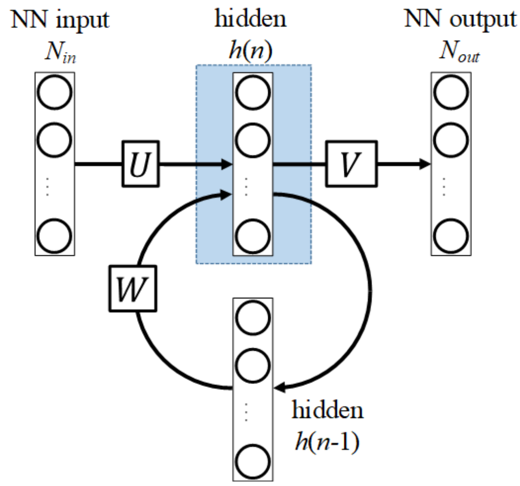

FIGURE 5. Structure of multi-layer recurrent neural network controller.

$$K_P = 1.2\frac{T}{\tau} \tag{2}$$

$$T_i = 0.5T \tag{3}$$

$$T_d = 2\tau \tag{4}$$

C. RNN WITH ADAM OPTIMIZATION ALGORITHM

In this paper, the multi-layer RNN controller is applied and the sum of the outputs of RNN and PID controllers is provided as the control input of the plant. In the proposed system, the RNN controller has three layers: one input layer, one hidden layer, and one output layer, as shown in Figure 5. The hidden layer has 10 neurons, and the structure of applied RNN controller is 3-10-1.

In this system, the reference value of the system y_{ref}, output temperature y, and the output of the feedforward compensator F_{out} are set as the input signals of the RNN. x_N is the output value of the RNN. The calculation process, from the input N_{in} to the output N_{out}, is shown in Figure 6, where U is the weight of input neurons, V is the weight of output neurons and W is state memory neurons' weight, and $f(\cdot)$ indicates the activation function of each neurons in the RNN controller. The output of RNN controller can be expressed as equation (5), where N_{in} is the input which includes output temperature$y$, temperature reference y_{ref}, and the feedforward compensator's output F_{out}. N_{out} is the output of the RNN controller, b indicates the offset value of the neurons in hidden layer, and c represents the bias of the neurons in the output layer.

$$N_{out} = V * f(f(U * N_{in}) + W * h(t-1) + b) + c \tag{5}$$

Regarding self-learning of the RNN controller, the Back Propagation Through Time (BPTT) calculation method is

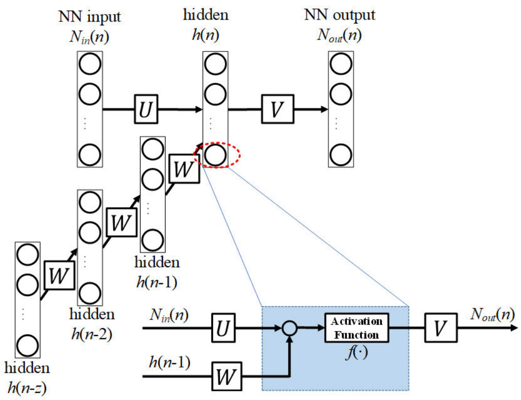

FIGURE 6. Calculation process for RNN controller.

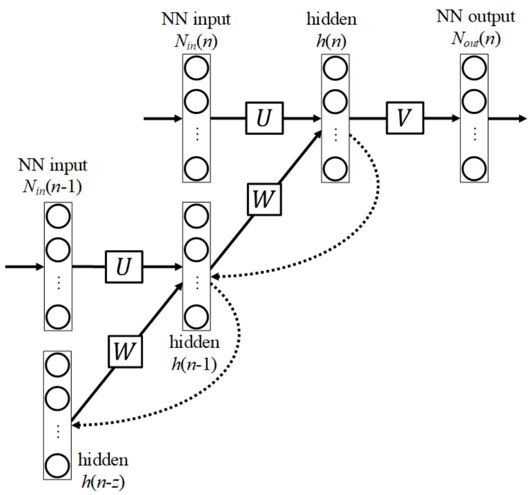

FIGURE 7. Back propagation through time (BPTT).

introduced for training and updating the weight and bias of each neuron, as seen in Figure 7. This is assuming that the RNN is working at the n^{th} calculation iterations ($n^{th} sampling period$) and the state memory layer has stored z steps of the previous calculation data.

The BPTT propagation starts from the output neuron of RNN controller. The learning signal of the neurons is provided by the error signal; thus, the gradient error at n^{th} calculation iteration can be represented as equation (6), where m indicates the number of output layer neurons.

$$E = \frac{1}{2}\sum_{i=1}^{m}(y_r(n) - y(n))^2. \tag{6}$$

Based on the gradient error, the local gradient for the output layer and hidden layer can be calculated as equations (7) and (8), respectively, where $u(n)$ and $o(n)$ are the induced local domain of the hidden layer and output layer, as represented in equations (9) and (10), respectively.

$$\delta_h(n) = \frac{\partial E}{\partial u(n)} = f'(u(n)) * V^T \delta_o(n) \tag{7}$$

$$\delta_o(n) = \frac{\partial E}{\partial o(n)} = f'(o(n)) * (y(n) - t(n)) \tag{8}$$

$$u(n) = U * N_{in}(n) + W * h(n-1) + b(n) \tag{9}$$

$$o(n) = V * h(n) + c(n) \tag{10}$$

Thus, for the z step stored calculation neurons, the local gradient from the n^{th} iteration to the $(n-z)^{th}$ iteration can be calculated as equation (11).

$$\delta_h(n-z-1) = \delta_h(n-z) * (W * f'(u(n-z-1))) \tag{11}$$

According to the BPTT algorithm, the corrections of U of the input layer can be expressed as equation (12), while the update of the weight V of the output layer can be calculated as equation (13), the weight correctness of the hidden layer as well as the memory neurons W is expressed in equation (14), α is the gain of weight training and updating, and can be optimized by the Adam algorithm which will be introduced later.

$$U(n+1) = U(n) - \triangle U = U(n) - \alpha \sum_{i=0}^{z} \delta_h(n-i) * N_{in}(n-i) \tag{12}$$

$$V(n+1) = V(n) - \triangle V = V(n) - \alpha \sum_{i=0}^{z} \delta_o(n) * h(n) \tag{13}$$

$$W(n+1) = W(n) - \triangle W = W(n) - \alpha \sum_{i=0}^{z} \delta_h(n-z) * h(n-z-1) \tag{14}$$

Weights aside, the bias of the neurons also needs to be updated for RNN performance. The updating of the hidden layer neuron bias b and output layer neuron bias c are determined by the local gradient of hidden layer $\delta_h(n)$ and output layer $\delta_o(n)$, respectively, which can be expressed as equations (15) and (16), respectively, where β represents the ratio of bias training and updating.

$$b(n+1) = b(n) - \beta \triangle b = b(n) - \beta \sum_{i=0}^{z} \delta_h(n-z) \tag{15}$$

$$c(n+1) = c(n) - \beta \triangle c = c(n) - \beta \sum_{i=0}^{z} \delta_o(n) \tag{16}$$

Based on the BPTT neuron weights and bias update obtained from above, to improve the learning efficiency of the RNN, *Adam* optimization is introduced to hold the term which is the exponentially damped average of the past slop square $\upsilon(n)$ and the slop $m(n)$ at n^{th} iteration. Assuming that $g(n)$ is the gradients of the neuron at at the n^{th} iteration (this situation is replaced by the teaching signal ${e_y}^2$)as expressed by equation (17), the calculation of the updating biased first

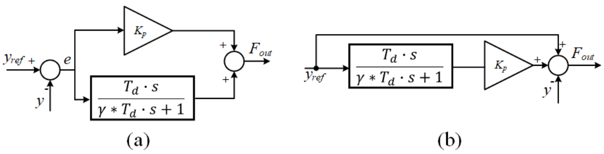

FIGURE 8. Structures of feedforward (FF) compensator: (a) PD structure, (b) 2DOF structure.

moment and second raw moment estimation can be expressed as equations (18) and (19), respectively, where β_1 and β_2 are the hyper-parameters of *Adam*.

$$g(n) = e_y^2 \tag{17}$$

$$m(n) = \beta_1 * m(n-1) + (1-\beta_1) * g(n) \tag{18}$$

$$\upsilon(n) = \beta_2 * \upsilon(n-1) + (1-\beta_2) * g^2(n) \tag{19}$$

Thus, the calculated bias-corrected first moment and second raw moment estimation can be expressed as equations (20) and (21), respectively. The final correction of the $\triangle w(n)$ can be expressed as equation (22), where $w(n)$ represents the weight matrix of one layer, α_{ad} is the step size of *Adam* calculation, and ε is the hyper-parameter of *Adam*. This correction will be applied to the weights U, V and W.

$$\hat{m}(n) = \frac{m(n)}{1-\beta_1^n} \tag{20}$$

$$\hat{\upsilon}(n) = \frac{\upsilon(n)}{1-\beta_2^n} \tag{21}$$

$$\triangle w(n) = -\frac{\alpha_{ad}}{sqrt\hat{\upsilon}(n) + \varepsilon} * \hat{m}(n) \tag{22}$$

By comparing different neuron activation functions, the *ReLu* function is applied as shown in equation (23), while its derivative function is expressed in equation (24).

$$f(x) = \begin{cases} x, & x > 0 \\ 0, & x \leq 0 \end{cases} \tag{23}$$

$$f'(x) = \begin{cases} 1, & x > 0 \\ 0, & x \leq 0 \end{cases} \tag{24}$$

D. FEED-FORWARD COMPENSATOR

In order to improve the performance of the RNN control and provide one kind of reference output for the RNN, the feedforward compensator *FF* is introduced to provide an extra input of the RNN controller. In this proposal, the type of PD and 2DOF(two degrees of freedom) compensators are considered, as presented in Figures 8(a,b), respectively. The parameters K_p, T_d are the same as those of the PID controllers' introduced above, and γ is the time constant gain of first order low pass filter(LPF) in the differential part of the PD controller, in this case, $\gamma = 0.5$.

E. REFERENCE MODEL

The reference model is calculated according to the identified real system mathematical transfer function and is introduced for providing a precise learning signal for the RNN controller. To ensure that the reference model can have exactly the same output characteristics as the real system, the pure time delay part of the plant needs to be approximated. There already exist several approximation methods, in this paper, the Padé approximation method is considered, shown as equation (25).

$$e^{-\tau s} \approx \frac{1}{(\frac{\tau}{2}s + 1)^2} \tag{25}$$

In this proposal, to improve the reference model response time, a gain R (smaller than 1) is introduced to the time constant component to shorten the response time of the reference model, as in equation (26). Approximation of dead time as a 2^{nd} order transfer function makes controller realization easy, i.e., it reduces the memory required to store the output.

$$R(s) \approx \frac{K}{T * R * s + 1} \times \frac{1}{(\frac{\tau s}{2} + 1)^2} \tag{26}$$

Further more, in this proposal, the reference model $R(s)$ is the ideal closed-loop transfer function the system want to achieve.Since it is not possible to achieve a response faster than the dead time of the controlled objects, $R(s)$ is set by adding (approximately) the dead time of the plant to a 2^{nd} order transfer function. Then, the NN controller compensates for the error between the actual output and the output from $R(s)$, by this way the efficiency of NN controller quick learning progress and system time response has been improved.

III. SIMULATION RESULTS

A. SYSTEM IDENTIFICATION BASED ON REAL EXPERIMENTAL PLATFORM

To evaluate the control effectiveness of the presented RNN control method, the controlled hotplate plant model should be calculated from a real temperature system. Thus, the system identification(step response method) experiments were carried out for the mathematical plant of the controlled single phase heating system. Figure 9 shows the platform of a 4-channel hotplate temperature control system. It is controlled by a digital signal processor (DSP) and has four hotplate temperature channels, while each channel is equipped with two semiconductor heaters and one wide range temperature sensor. The transfer ratio between input temperature and output voltage of the temperature sensor is 0.025 (the sensor can transfer 0-400 $°C$ temperature to 0-10 *VDC* voltage). The heaters are driven by pulse width modulation(PWM) signals. The temperature can be controlled through the duty ratio of the PWM signals.

In this proposal, the single phase hotplate temperature control system is defined as the input channel being Ch1 and the output channel being Ch4. The SISO temperature system control object transfer function can be identified as equation (27).

$$P(s) = \frac{2.854}{2395s + 1} e^{-444.74s} \tag{27}$$

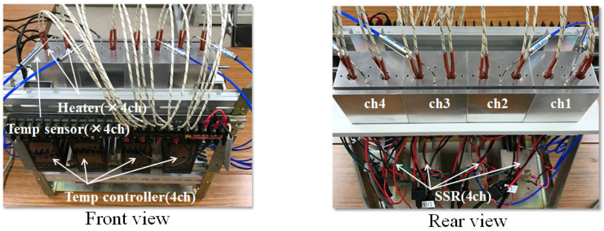

FIGURE 9. Experimental platform.

B. SIMULATIONS AND RESULTS ANALYSIS

The model of system simulation was developed using MATLAB software. In simulations, the transfer function of the controlled object was the same as that expressed in equation (27). Thus, the calculated and approximated reference model can be obtained as equation (28), where, R is set as 0.01.

$$R(s) \approx \frac{2.854}{0.01 * 2395s + 1} \times \frac{1}{(\frac{444.74}{2}s + 1)^2} \tag{28}$$

The traditional IPD controller parameters are obtained using the Z-N method. Here, the controller parameters were calculated as $K_p = 2.264$, $T_i = 889.48$, and $T_d = 222.37$. In addition, the RNN parameters were defined by testing method as $\alpha = 1 \times 10^{-9}$ and $\beta = 1 \times 10^{-3}$. The initial neuron weight was determined under random and limitation rule to be an optimal (random) value. The memory store steps $z = 10$, the hyper parameters of the Adam calculation were defaulted as $\beta_1 = 0.99$, $\beta_2 = 0.99958$, $\varepsilon = 1 \times 10^{-20}$.

The simulation comprises two phases. Phase 1 was the reference value tracking response. Phase 2 was the reference value response with disturbance variation. Both phases have two parts: Part 1 is RNN training and initial state control; Part 2 is bidirectional reference tracking (positive and negative direction temperature control). In Part 1, the output temperature rises from 0 $°C$ to 100 $°C$, and the main control action switches from PID to RNN controller. In Part 2, the reference value of the output temperature is given as a repetitive step signal with an amplitude of 5$°C$, and the offset of the reference is 100$°C$. The positive direction temperature control is defined by controlling output temperature from 100$°C$ to 105$°C$, while the negative direction temperature control is defined by controlling output temperature from 105$°C$ to 100$°C$. For disturbance variation in Phase 2, a 20% disturbance was added to the control input of the plant when the system reached a steady state in the bidirectional control period. The RNN controller with PD feedforward compensator (define as PD3INN) and a 2DOF feedforward compensator (2DOF3INN) was simulated and the results were against those of traditional IPD temperature control system in terms of quantity.

1) PHASE 1: REFERENCE TRACK SIMULATION RESULTS

Figures 10 (a,b) respectively show the output temperature reference tracking response of the controlled system and both positive temperature tracking (temperature increase from 100$°C$ to 105$°C$) and negative temperature tracking (temperature decrease from 105$°C$ to 100$°C$) results of the PD3INN system, and are compared with the results obtained by only equipping a traditional IPD control system.

From the simulation results, for the positive direction temperature response, the rising time of the IPD control system is about 1101s, while that of the PD3INN control system is only 598.5s; therefore, the temperature rising time has been shortened by 46%. The traditional IPD system has a settling time of around 3587s but only 993.0s for the PD3INN control system; thus, the system settling time has been increased by 73%. Furthermore, the traditional IPD system has an overshoot of around 0.5$\circ C$(10% of the reference value), while the PD3INN has no overshoot. For the negative direction temperature tracking, the dropping time of the traditional IPD system is around 1100s and the dropping time

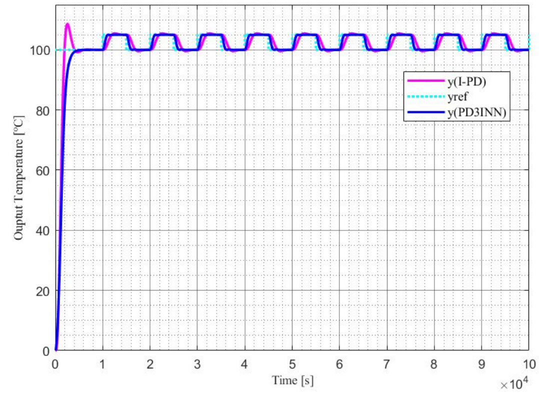

(a)

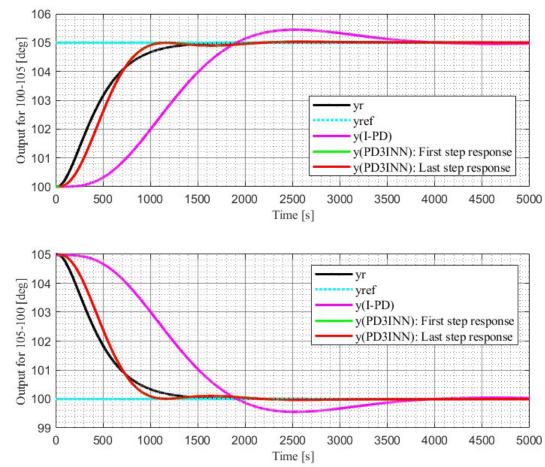

(b)

FIGURE 10. Simulation results.(a) Full time response for PD3INN controlled system and (b) positive temperature output results (temperature increase from 100°C to 105°C) and negative temperature output results (temperature decrease from 105°C to 100°C) direction of presented PD3INN control system and traditional IPD temperature system.

of PD3INN control system is only 598s, so the temperature dropping time has been shortened by 46%; the settling time for the IPD control system is around 3587s, where as for the PD3INN control system the settling time is only 993.0s, representing a decrease of 73%. Furthermore, the traditional IPD control system has an undershoot of around 0.5°C(10% of the temperature reference value), while the PD3INN has no undershoot. In addition, from the results of temperature tracking for repetitive reference value, for both temperature rising and dropping steps, the last rising and dropping step are almost the same as the first rising and dropping step. We can conclude that the RNN controller has finished its self-learning progress before the first rising and dropping step, and quick training of RNN has been realized. These comparison results successfully confirmed that the system performance was enhanced by the PD3INN control system.

Figures 11 (a,b) respectively show the output temperature reference tracking response of the controlled system and both positive temperature tracking (temperature rise from 100∘C to 105°C)and negative temperature tracking (temperature drop from 105°C to 100°C) results of the 2DOF3INN system, and a comparison with the results obtained by only equipping a traditional IPD control system.

From the simulation results, for the positive direction temperature response, the rising time of the IPD control system is about 1101s, while that of the 2DOF3INN control system is only 645.5s; so, the temperature rising time has been reduced by 41%. The conventional IPD system has a settling time of around 3587s but 2526.5s for the 2DOF3INN control system; thus, the system settling time has been increased by 30%. Furthermore, the traditional IPD system has an overshoot of around 0.5°C(10% of the reference value), while the 2DOF3INN has no overshoot. For the negative direction temperature tracking, the dropping time of the traditional IPD system is around 1100s and the dropping time of 2DOF3INN control system is only 645s, so the temperature dropping time has been reduced by 41%; the settling time of the IPD control system is around 3587s, where for the 2DOF3INN control system it is only 2526s, so the settling time has been shortened by 30%. The traditional IPD control system has an undershoot of around 0.5°C(10% of the temperature reference value), while the 2DOF3INN has no undershoot.

In addition, from the results of temperature tracking for repetitive reference value, for both temperature rising and dropping steps, the last rising and dropping step are almost the same as the first rising and dropping step. We can thus conclude that the RNN controller has finished its self-learning progress before the first rising and dropping step, and quick training of RNN has been realized. These comparison results successfully confirmed that the system performance has been enhanced by the 2DOF3INN control system.

A full comparison of the positive direction reference tracking efficiency of these three control systems is shown in Table 1, and a comparison of the negative direction reference tracking efficiency of the systems is shown in Table 2. As a result, the improvement is the same in both positive direction control and negative direction control, and the performance of the PD3INN control system is better than that of the 2DOF3INN control system.

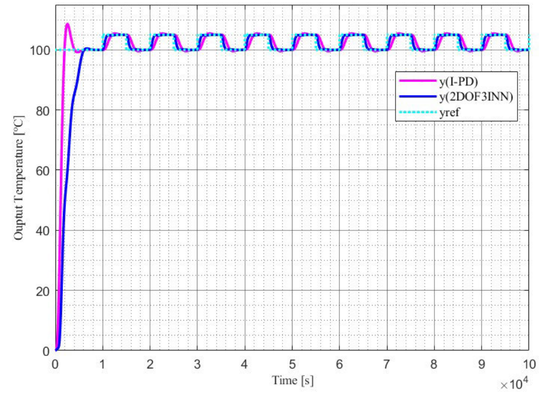

(a)

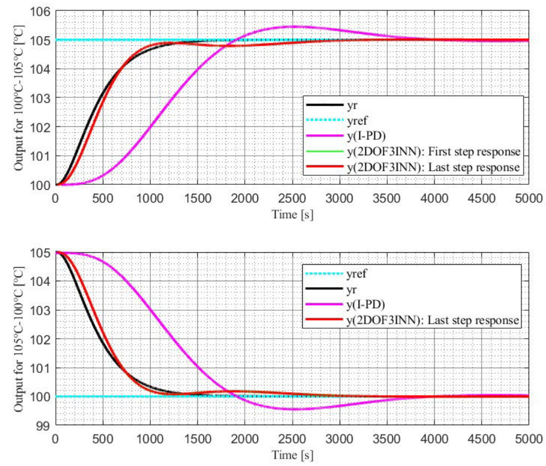

(b)

FIGURE 11. Simulation results.(a) Full time response for 2DOF3INN controlled system and (b) positive temperature output results (temperature rising from 100°C to 105°C) and negative temperature output results (temperature dropping from 105°C to 100°C) direction of presented 2DOF3INN control system and traditional IPD temperature system.

TABLE 1. Efficiency comparison of temperature rising from 100°C to 105°C. (Source: after own calculation.)

	IPD	PD3INN	2DOF3INN
Rising time T_r [s]	1101(100 %)	598(54.4 %)	645(58.7 %)
2 % setting time T_r [s]	3587(100 %)	993(27.6 %)	2526(70.4 %)
Overshoot[°C]	0.5(10 %)	0(0 %)	0(0 %)

2) PHASE 2: DISTURBANCE VARIATION SIMULATION RESULTS

In this case, an amplitude of 20% disturbance was added to the control input after the system reached a steady-state in

TABLE 2. Efficiency comparison of temperature dropping from 105°C to 100°C.(Source: after own calculation.)

	IPD	PD3INN	2DOF3INN
Dropping time T_d $[s]$	1101(100 %)	598(54.4 %)	645(58.7 %)
2 % setting time T_s $[s]$	3587(100 %)	993(27.6 %)	2526(70.4 %)
Undershoot$[°C]$	0.5(10 %)	0(0 %)	0(0 %)

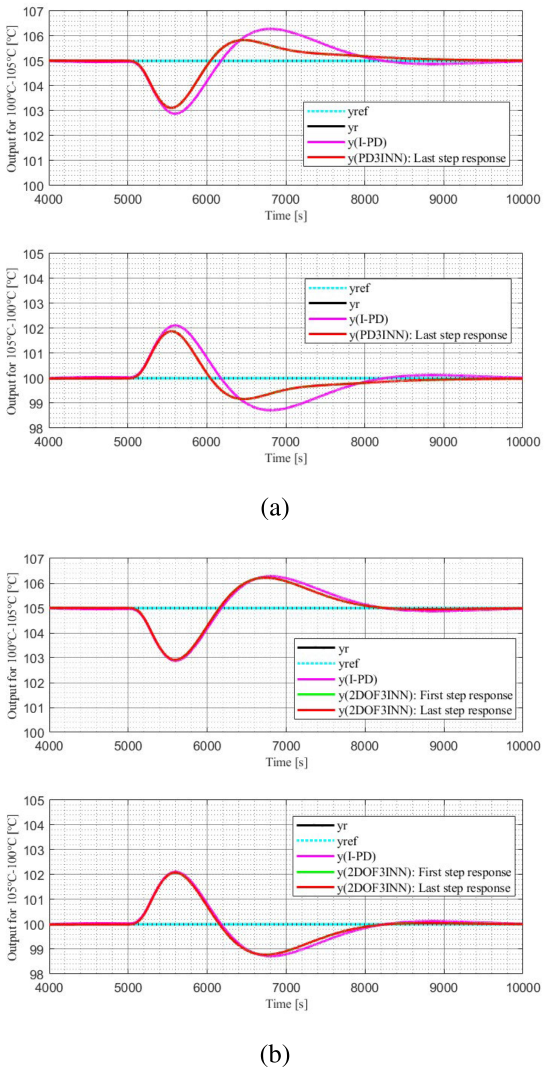

FIGURE 12. Bidirectional disturbance response simulation results. (a) Bidirectional disturbance response of PD3INN control system and (b) Bidirectional disturbance response of 2DOF3INN control system.

both positive and negative direction controls. The bidirectional disturbance response of the PD3INN and 2DOF3INN control systems is shown in Figures 12(a,b), respectively.The results of the traditional IPD control system are also shown for comparison in both kinds of direction tracking.

From the simulation results, the 20% disturbance is added at the time 5000s. The analysis of the simulation results focused on the temperature drop for positive direction state and the temperature increase for negative direction state. We also added the settling time of the system after disturbance and the overshoot for positive and undershoot

TABLE 3. Disturbance response comparison of temperature rising from 100°C to 105°C. (Source: after own calculation.)

	IPD	PD3INN	2DOF3INN
Temperature drop $[°C]$	2.12(100 %)	1.90(89.6 %)	2.08(98.1 %)
2 % setting time T_s $[s]$	4235(100 %)	3500(82.6 %)	2998(70.8 %)
Overshoot$[°C]$	1.25(25 %)	0.87(17.15 %)	1.23(24.46 %)

TABLE 4. Disturbance response comparison of temperature rising from 105°C to 100°C. (Source: after own calculation.)

	IPD	PD3INN	2DOF3INN
Temperature increase $[°C]$	2.12(100 %)	1.90(89.6 %)	2.08(98.1 %)
2 % setting time T_s $[s]$	4235(100 %)	3498(82.61 %)	3000(70.3 %)
Overshoot$[°C]$	1.26(25.2 %)	0.85(17 %)	1.22(24.4 %)

for negative response to the disturbance. For the positive direction control, after the disturbance was added, the temperature drop of the conventional I-PD control system was 2.12°C, while that of the PD3INN and 2DOF3INN control systems was 1.9°C and 2.08°C, respectively. Thus the dropping temperature caused by the disturbance has been decreased with PD3INN and 2DOF3INN systems by around 11% and 2%, respectively. The settling time after the disturbance added to the IPD system is about 4235.5s, and that of the PD3INN and 2DOF3INNcontrol systems are 3500s and 2998.5s, respectively. The settling time was respectively improved by17.4% and 29.2%. Moreover, the IPD has an overshoot of 1.25°C, while only 0.87°C for the PD3INNcontrol system and 1.23°C for the 2DOF3INN control system.

For the negative direction control, after the disturbance was added, the temperature increase of the conventional IPD control system was 2.12°C, while that of the PD3INN and 2DOF3INNcontrol systems was 1.86°C and 2.05°C, respectively. Thus the dropping temperature caused bythe disturbance was decreased with the PD3INN and 2DOF3INN systems by around 11% and 2%, respectively. The setting time after the disturbance was added to the I-PD system was about 4235 s, and that of the PD3INN and 2DOF3INN control systems was 3498.5 s and 3000.5 s, respectively. The setting time was respectively improved by 17.4% and 29.2%. Moreover, the I-PD has an overshoot of 1.25°C, while only 0.85°C for the PD3INN control system and 1.22°C for the 2DOF3INN control system,respectively. Thus, the disturbance of the positive direction control is almost the same as the negative direction control, and both PD3INN and 2DOF3INN control systems improved the control efficiency of the disturbance response. A full comparison of the positive direction disturbance responses of these three control systems is shown in Table 3, and a comparison of the negative direction disturbance responses is shown in Table 4.

IV. EXPERIMENTS AND RESULTS ANALYSIS

To further evaluate the RNN with the Adam optimization control method for the single phase hotplate temperature system, experiments needed to be carried out. The parameters (including controller parameters and model parameters) were

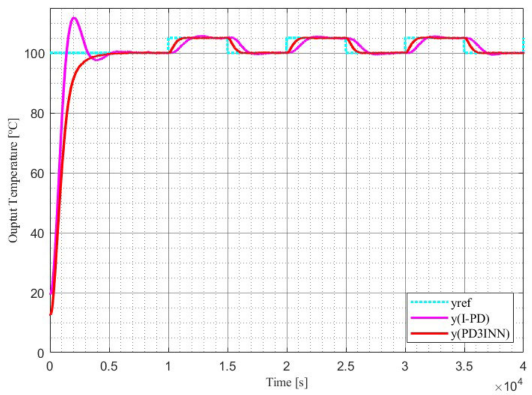

(a)

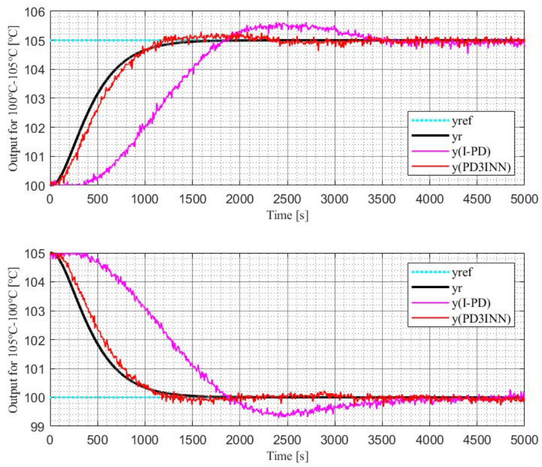

(b)

FIGURE 13. **(a) Full time response for PD3INN controlled system and (b) positive temperature output results (temperature increase from 100°C to 105°C) and negative temperature output results (temperature decrease from 105°C to 100°C) of presented PD3INN system with the traditional IPD temperature system).**

exactly the same as those applied in simulations.The platform for experiments was the same as the system identification experiment platform as shown in Figure 8. According to the comparative results of the simulation, the PD3INN has better performance both in reference tracking and disturbance response; thus, experiments were carried using the PD3INN control structure. As with the simulations, the experiments were divided into two phases: Phase 1 was reference tracking experiments; Phase 2 was disturbance response experiments. The results had to be compared with a traditional IPD control system to evaluate the control performance and effectiveness of the PD3INN system.

A. PHASE 1: REFERENCE TRACKING EXPERIMENTS

In the case of these experiments, the temperature was first controlled from room temperature(about 20°C) to initial state (100°C); this stage is called RNN self-learning and initial state control. After this initial state, the reference

TABLE 5. **Efficiency comparison of temperature rising from 100°C to 105°C. (Source: after own calculation.)**

	IPD	PD3INN
Rising time T_r $[s]$	1098(100 %)	743(68 %)
2 % setting time T_s $[s]$	3036(100 %)	1050(33 %)
Overshoot$[°C]$	0.6(12 %)	0(0 %)

TABLE 6. **Efficiency comparison of temperature rising from 105°C to 100°C. (Source: after own calculation.)**

	IPD	PD3INN
Dropping time T_d $[s]$	1097(100 %)	744(67 %)
2 % setting time T_s $[s]$	3033(100 %)	1055(36.7 %)
Undershoot$[°C]$	0.6(12 %)	0(0 %)

was changed as a repetitive step signal with an amplitude of 5°C, and the offset of the reference was 100°C. The positive temperature control is defined by the controlling output temperature rising from 100°C to 105°C, while the negative temperature control is defined by the controlling output temperature dropping from 105°C to 100°C. Figures 13(a,b) show the full time response of the controlled system and the results of both positive (temperature rising from 100°C to 105°C) and negative (temperature dropping from 105°C to 100°C) direction control of the PD3INN system, respectively. These results were compared with those obtained from a traditional IPD control system with the same control parameters.

From the experiment results, for the positive direction temperature response, the rising time of the IPD control system is about 1098s, while that of the PD3INN control system is only 743s; thus, the temperature rising time has been shortened by 32%. The traditional IPD system has a settling time of around 3036s while only 1050s for PD3INN control system, thus the system settling time has been increased by 66%. Further more, the traditional IPD system has an overshoot of around 0.6°C(10% of the reference value) while the PD3INN system has no overshoot.

For the negative direction temperature tracking, the dropping time of the traditional IPD system is around 1097s and the dropping time of PD3INN control system is only 744s, so the temperature dropping time has been reduced by 33%; the settling time for the IPD control system is around 3036s, where as for the PD3INN control system it is only 1050s, so the settling time has been reduced by 63.3%. The traditional IPD control system has an undershoot of around 0.6°C (12% of the temperature reference value), while the PD3INN has no undershoot. The comparative results of positive and negative direction control are shown in Tables 5 and 6, respectively. Thus, the simulation and experimental results both verify the proposed PD3INN control method.

B. PHASE 2: DISTURBANCE RESPONSE EXPERIMENTS

In this case, an amplitude of 20% disturbance was added to the control input after the system reached a steady-state in

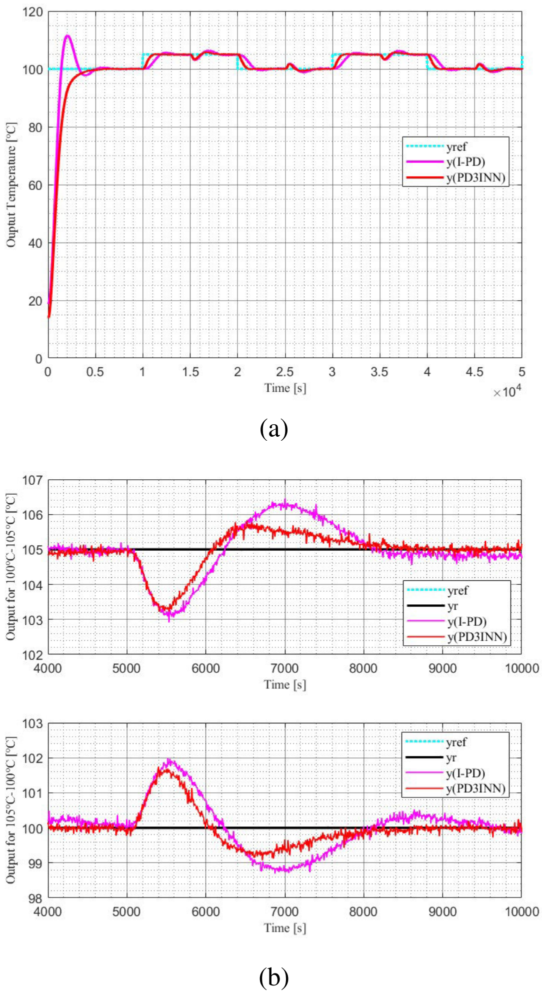

FIGURE 14. Experimental results. (a) Full time response for PD3INN controlled system and (b)Bidirectional disturbance response of PD3INN system and traditional IPD system.

both positive and negative direction control. Figures 14 (a,b) respectively show the full time response of the controlled system and the disturbance response results in positive and negative direction control and compared to those results obtained from the conventional IPD control system.

From the experimental results, the 20% disturbance was added at time 5000s. For the positive direction control, after the disturbance was added, the temperature drop of the traditional IPD control system was 1.9°C, while that of the PD3INN was 1.7°C; thus, the temperature dropping value decreased by 10%. The settling time after the disturbance was added to the IPD system was around 2930s, while that of PD3INN was 2815s. The setting time was increased by 4%. Furthermore, the IPD has an overshoot of 1.3°C, but 0.7°C for the PD3INN control system, so the overshoot successfully decreased by 12%.

For the negative direction control, after the disturbance was added, the temperature increase of the conventional IPD control system is 1.9°C, while that of the PD3INN is 1.68°C; thus,the temperature decreased with PD3INN by about 12%. The settling time after the disturbance was added to the IPD system was about 2940s, while that of PD3INN was 2810.5s. The setting time increased by 4.4%. The IPD had an undershoot of 1.3°C, but only 0.7°C for the PD3INN control system, so the undershoot decreased by 12%. The comparative results are shown in Table 6. Thus, the disturbance of the positive direction control is almost the same as the negative direction control, and both simulation and experimental results have successfully verified the control efficiency of the introduced RNN with the Adam optimization control method.

TABLE 7. Disturbance response comparison of temperature increase from 100°C to 105°C.(Source: after own calculation.)

	IPD	PD3INN
Temperature drop [°C]	1.9(100 %)	1.7(90 %)
2 % setting time T_s [s]	2930(100 %)	2815(96 %)
Overshoot[°C]	1.3(26 %)	0.7(14 %)

TABLE 8. Disturbance response comparison of temperature increase from 105°C to 100°C. (Source: after own calculation.)

	IPD	PD3INN
Temperature increase [°C]	1.9(100 %)	1.68(88 %)
2 % setting time T_s [s]	2940(100 %)	2810(95.6 %)
Undershoot[°C]	1.3(26 %)	0.7(14 %)

V. CONCLUSION

In this brief, an RNN controller with an *Adam* optimization algorithm suitable for single phase hotplate temperature control systems was proposed. The control system is driven by the error signal between the system output and the reference model output. The RNN system was combined with PID control.Two types of feedforward compensators (PD and 2DOF) were introduced to improve the performance of the RNN controller. The proposed design was applied to a FOPTD plant. Simulations of both reference tracking and disturbance response were run in a MATLAB environment. Simulation results of reference tracking and disturbance response in both directions were presented and compared with those obtained from a traditional IPD control system using the same parameters. Experiments for the PD3INN system were performed on a digital controlled temperature platform. The comparative results with a traditional IPD control system allowed for a successfully evaluation of improvements in reference tracking time, system settling time, overshoot, and disturbance response of the single phase hotplate temperature control system.Due to the limitations of the proposed system, in that it depends on the adjustment of hyper parameters, and the versatility and control performance of the control system are restricted, the future work of this research will focus on a pruning optimization method and verification of generalization for parameter fluctuations of controlled objects.

REFERENCES

[1] N. Suda, *PID Control*. Tokyo, Japan: Asakura, 1992.

[2] M. Oshima, *Process Control Systems*. New York, NY, USA: Corona, 2003.

[3] G. C. Goodwin, S. F. Fraebe, and M. E. Salgado, *Control System Design*. Upper Saddle River, NJ, USA: Prentice-Hall, 2001.

[4] M. Morari and E. Zafiriou, *Robust Process Control*. Upper Saddle River, NJ, USA: Prentice-Hall, 1992.

[5] J. M. Maciejowski, *Multivariable Feedback Design*. Boston, MA, USA: Addison Wesley, 1989.

[6] J.-S. Ko, J.-H. Huh, and J.-C. Kim, "Improvement of temperature control performance of thermoelectric dehumidifier used Industry 4.0 by the SF-PI controller," *Processes*, vol. 7, no. 2, p. 98, Feb. 2019, doi: 10.3390/pr7020098.

[7] X. Xiao, H. Xue, and B. Chen, "Nonlinear model for the dynamic analysis of a time-dependent vehicle-cableway bridge system," *Appl. Math. Model.*, vol. 90, pp. 1049–1068, Feb. 2021.

[8] A. Fujimori and S. Ohara, "Order reduction of plant and controller in closed loop identification based on joint input-output approach," *Int. J. Control, Autom. Syst.*, vol. 15, no. 3, pp. 1217–1226, Jun. 2017.

[9] Y. Yao, K. Yang, M. Huang, and L. Wang, "A state-space model for dynamic response of indoor air temperature and humidity," *Building Environ.*, vol. 64, pp. 26–37, Jun. 2013.

[10] X. Chen, Z. Mao, and R. Jia, "A new multiple kernel-based regularization method for identification of delay linear dynamic systems," *Chemometric Intell. Lab. Syst.*, vol. 199, Apr. 2020, Art. no. 103971.

[11] V. Feliu-Batlle and R. Rivas-Perez, "Control of the temperature in a petroleum refinery heating furnace based on a robust modified Smith predictor," *ISA Trans.*, vol. 112, pp. 251–270, Jun. 2021.

[12] J. Bai, S. Wang, and X. Zhang, "Development of an adaptive Smith predictor-based self-tuning PI controller for an HVAC system in a test room," *Energy Buildings*, vol. 40, no. 12, pp. 2244–2252, Jan. 2008.

[13] M. Xu and S. Li, "Practical generalized predictive control with decentralized identification approach to HVAC systems," *Energy Convers. Manag.*, vol. 48, no. 1, pp. 292–299, Jan. 2007.

[14] J. Zhang, X. Li, T. Zhao, and W. Dai, "Experimental study on a novel fuzzy control method for static pressure reset based on the maximum damper position feedback," *Energy Buildings*, vol. 108, pp. 215–222, Dec. 2015.

[15] A. Afram and F. Janabi-Sharifi, "Theory and applications of HVAC control systems—A review of model predictive control (MPC)," *Building Environ.*, vol. 72, pp. 343–355, Feb. 2014.

[16] Z. Gao, S. K. Nguang, and D. X. Kong, "Guest editorial: Special section on data-driven approaches for complex industrial systems," *IEEE Trans. Ind. Informat.*, vol. 9, no. 4, pp. 2210–2212, Nov. 2013.

[17] Z. Gao, S. K. Nguang, and D.-X. Kong, "Advances in modelling, monitoring, and control for complex industrial systems," *Complexity*, vol. 2019, Feb. 2019, Art. no. 2975083, doi: 10.1155/2019/2975083.

[18] S. H. Ryu and H. J. Moon, "Development of an occupancy prediction model using indoor environmental data based on machine learning techniques," *Building Environ.*, vol. 107, pp. 1–9, Oct. 2016.

[19] A. C. Megri and I. El Naqa, "Prediction of the thermal comfort indices using improved support vector machine classifiers and nonlinear kernel functions," *Indoor Built Environ.*, vol. 25, no. 1, pp. 6–16, Feb. 2016.

[20] R. Badia-Melis, U. McCarthy, and I. Uysal, "Data estimation methods for predicting temperatures of fruit in refrigerated containers," *Biosyst. Eng.*, vol. 151, pp. 251–272, Nov. 2016.

[21] S. Mercier, B. Marcos, and I. Uysal, "Identification of the best temperature measurement position inside a food pallet for the prediction of its temperature distribution," *Int. J. Refrigeration*, vol. 76, pp. 147–159, Apr. 2017.

[22] S. Jebamalar, J. J. Christopher, and M. A. T. Ajisha, "Random input based prediction and transfer of heat in soil temperature using artificial neural network," *Mater. Today, Proc.*, vol. 45, pp. 1540–1546, Jan. 2021.

[23] M. C. Nunes, M. Nicometo, J. P. Emond, R. B. Melis, and I. Uysal, "Improvement in fresh fruit and vegetable logistics quality: Berry logistics field studies," *Phil. Trans. Roy. Soc. A, Math., Phys. Eng. Sci.*, vol. 372, no. 2022, Aug. 2014, Art. no. 20140212.

[24] V. Raab, B. Petersen, and J. Kreyenschmidt, "Temperature monitoring in meat supply chains," *Brit. Food J.*, vol. 113, no. 10, pp. 1267–1289, Sep. 2011.

[25] K. Katić, R. Li, J. Verhaart, and W. Zeiler, "Neural network based predictive control of personalized heating systems," *Energy Buildings*, vol. 174, pp. 199–213, Sep. 2018.

[26] X. Li, T. Zhao, J. Zhang, and T. Chen, "Predication control for indoor temperature time-delay using Elman neural network in variable air volume system," *Energy Buildings*, vol. 154, pp. 545–552, Nov. 2017.

[27] S. Mercier and I. Uysal, "Neural network models for predicting perishable food temperatures along the supply chain," *Biosyst. Eng.*, vol. 171, pp. 91–100, Jul. 2018.

[28] I. Chakroun, T. Haber, and T. J. Ashby, "SW-SGD: The sliding window stochastic gradient descent algorithm," *Proc. Comput. Sci.*, vol. 108, pp. 2318–2322, Jan. 2017.

[29] H. Bao, J. Feng, N. Dinh, and H. Zhang, "Deep learning interfacial momentum closures in coarse-mesh CFD two-phase flow simulation using validation data," *Int. J. Multiphase Flow*, vol. 135, Feb. 2021, Art. no. 103489.

[30] Z. Fei, Z. Wu, Y. Xiao, J. Ma, and W. He, "A new short-arc fitting method with high precision using Adam optimization algorithm," *Optik*, vol. 212, Jun. 2020, Art. no. 164788.

[31] F. Godin, J. Degrave, J. Dambre, and W. De Neve, "Dual rectified linear units (DReLUs): A replacement for tanh activation functions in quasi-recurrent neural networks," *Pattern Recognit. Lett.*, vol. 116, pp. 8–14, Dec. 2018.

[32] M. Tanaka, "Weighted sigmoid gate unit for an activation function of deep neural network," *Pattern Recognit. Lett.*, vol. 135, pp. 354–359, Jul. 2020.

[33] K. Eckle and J. Schmidt-Hieber, "A comparison of deep networks with ReLU activation function and linear spline-type methods," *Neural Netw.*, vol. 110, pp. 232–242, Feb. 2019.

[34] G. Lin and W. Shen, "Research on convolutional neural network based on improved ReLU piecewise activation function," *Proc. Comput. Sci.*, vol. 131, pp. 977–984, Jan. 2018.

[35] S. Masood and P. Chandra, "Training neural network with zero weight initialization," in *Proc. CUBE Int. Inf. Technol. Conf.*, Sep. 2012, pp. 235–239, doi: 10.1145/2381716.2381761.

[36] S. Lu, S.-H. Wang, and Y.-D. Zhang, "Detecting pathological brain via ResNet and randomized neural networks," *Heliyon*, vol. 6, no. 12, Dec. 2020, Art. no. e05625.

[37] S. Masood, M. N. Doja, and P. Chandra, "Analysis of weight initialization methods for gradient descent with momentum," in *Proc. Int. Conf. Soft Comput. Techn. Implementations (ICSCTI)*, Oct. 2015, pp. 131–136.

[38] S. Krishna Kumar, "On weight initialization in deep neural networks," 2017, *arXiv:1704.08863*.

[39] O. C. Yolcu, F. A. Temel, and A. Kuleyin, "New hybrid predictive modeling principles for ammonium adsorption: The combination of response surface methodology with feed-forward and Elman-recurrent neural networks," *J. Cleaner Prod.*, vol. 311, Aug. 2021, Art. no. 127688.

[40] O. Pauca, A. Maxim, and C.-F. Caruntu, "Control architecture for cooperative autonomous vehicles driving in platoons at highway speeds," *IEEE Access*, vol. 9, pp. 153472–153490, 2021.

[41] L. F. C. Ccari and P. R. Yanyachi, "A novel neural network-based robust adaptive formation control for cooperative transport of a payload using two underactuated quadcopters," *IEEE Access*, vol. 11, pp. 36015–36028, 2023.

[42] J. Zhang, X. Wang, and L. Ma, "A finite-time distributed cooperative control approach for microgrids," *CSEE J. Power Energy Syst.*, vol. 8, no. 4, pp. 1194–1206, Jul. 2022.

[43] R. Gao and Z. Gao, "Pitch control for wind turbine systems using optimization, estimation and compensation," *Renew. Energy*, vol. 91, pp. 501–515, Jun. 2016.

[44] S.-D. Lee, S.-S. You, X. Xu, and T. N. Cuong, "Active control synthesis of nonlinear pitch-roll motions for marine vessels," *Ocean Eng.*, vol. 221, Feb. 2021, Art. no. 108537.

[45] J. G. Ziegler, N. B. Nichols, and N. Y. Rochester, "Optimum settings for automatic controllers," *Trans. ASME*, vol. 64, pp. 759–768, Nov. 1942.

SONG XU (Member, IEEE) was born in Zhenjiang, China, in 1991. He received the B.S. and M.S. degrees (Hons.) from the College of Electrical, Energy and Power Engineering, Yangzhou University, Yangzhou, China, in 2014 and 2017, respectively, and the Ph.D. degree from the Division of Electronics and Informatics, College of Science and Technology, Gunma University, Kiryu, Gunma, Japan, in 2020.

From March 2020 to October 2020, he was a Foreign Researcher with Gunma University. In 2020, he joined the Jiangsu University of Science and Technology, where he is currently a Lecturer with the College of Automation. His current research interests include big data compression, digitalized power transfer to renewable energy and energy storage devices, and intelligent control applications in industrial processes.

Dr. Xu's awards and honors include the three times ''Best Presentation Award'' of International Conference ICMEMIS, in 2017, 2018, and 2019, respectively. The second prize of Yangzhou Natural Science Outstanding Paper Award and Second Prize of Science and Technology Progress Award of Jiangsu Cold Chain Society.

SIYUAN SHI was born in Suqian, Jiangsu, China, in 2000. He received the bachelor's degree in electrical engineering and its automation from the Jiangsu University of Science and Technology, Jiangsu, in 2022, where he is currently pursuing the master's degree.

His current research interests include power transfer to renewable energy and energy storage devices, and their applications for smart grid.

WEI JIANG (Member, IEEE) was born in Yangzhou, China, in 1980. He received the B.S.E.E. degree from Southwest Jiaotong University, Chengdu, China, in 2003, and the M.Sc. and Ph.D. degrees in electrical engineering from The University of Texas at Arlington, TX, USA, in 2006 and 2009, respectively.

From 2007 to 2008, he was a Senior Design Engineer with EF Technologies L.L.C., TX. In 2010, he joined Yangzhou University and founded the Smart Energy Laboratory, where he is currently a Professor. He has been a Visiting Professor with Gunma University, Japan, in 2012, University of Strathclyde, and Aston University, U.K., in 2015. He holds two U.S. patents and 15 Chinese patents with two licensed by the industry. His current research interests include digitalized power conditioning to renewable energy and energy storage devices and the microscopic analysis of electromechanical energy conversion.

Dr. Jiang was the four-time Yangzhou University Excellent Teaching Award Winner.

SEIJI HASHIMOTO (Member, IEEE) was born in Aomori, Japan, in 1971. He received the M.E. and Ph.D. degrees in electrical and electronic engineering from Utsunomiya University, Japan, in 1996 and 1999, respectively.

He joined the Department of Mechanical Engineering, Oyama National College of Technology. Since 2002, he has been a Research Associate with the Department of Electronic Engineering, Gunma University, where he is currently a Professor with the Division of Electronics and Informatics. He has consulted for companies in control and energy applications and he has been a visitor professor in China. His research interests include system identification, motion control, intelligent control, and its application to industrial fields.